Article

Modelling, identification and structural damage investigation of the Neoria monument in Chania

Charalambidi, Barbara, Koutsianitis, Panagiotis, Motsa, Siphesihle Mpho, Tairidis, Georgios, Kasampali, Amalia, Drosopoulos, Georgios, Stavroulaki, Maria and Stavroulakis, Georgios

Developments in the Built Environment 10 (2022) 100069

Contents lists available at ScienceDirect

Developments in the Built Environment

journal homepage: www.sciencedirect.com/journal/developments-in-the-built-environment

Modelling, identification and structural damage investigation of the Neoria monument in Chania

Barbara Charalambidi [a,1], Panagiotis Koutsianitis [a,1], Siphesihle Mpho Motsa [b], Georgios Tairidis [a], Amalia Kasampali [a,1], Georgios Drosopoulos [b,c], Maria Stavroulaki [a,1], Georgios Stavroulakis [a,1,*]

[a] Technical University of Crete, Chania, 73100, Greece
[b] University of Kwazulu-Natal, Durban, South Africa
[c] University of Central Lancashire, Preston, United Kingdom

ARTICLE INFO

Keywords:
Finite element analysis
Monuments
Modal assurance criterion
Pushover analysis
Damage evaluation
Performance prediction

ABSTRACT

The structural behavior of Neoria masonry monument is studied here. The determination of structural and material properties of a partially collapsed monument and the evaluation of existing damages and their importance for further restoration studies are not trivial tasks. The investigation has been based on detailed geometric data, collected from sources and in-situ measurements. For the mechanical analysis, finite element models have been created with different level of detail, including simplified description of documented damages. Modal analysis is assisted by micro-tremor measurements. Comparison of the predictions with the experimentally measured quantities, allows the determination of material parameters with higher accuracy. A least square technique assisted by the modal assurance criterion has been used, by driving the model from a Python script. A comparison of collapse predictions based on modified pushover analysis, with classical modal analysis has been performed. An explanation of existing damages is attempted, based on the numerical models.

1. Introduction

Masonry arches are among the oldest structural systems in the world. The technique of building masonry arches was first seen in the 2nd millennium BC in Mesopotamian brick architecture (Anastasio, 2020). Arches develop their strength by transferring the applied load into compressive forces, in a thrust line along adjacent masonry blocks (Chilton and Isler, 2020). When the thrust line is found out of the section of the masonry blocks, opening of the interfaces between the blocks takes place which can result in a hinge collapse mechanism (Heyman, 1982). Furthermore, compressive failure is unlikely on masonry arch structures. Masonry structures in general have a peculiar mechanical behavior due to their no-tension material characteristics. Form of the structure and mechanics are working together, in order all parts are mainly in compression. This can be changed from settlement movement or earthquake loadings so activation of interfaces, damages and eventually partial or total collapse are presented. Detailed structural analysis including unilateral interfaces and cracks is, in principle, possible (Leftheris et al., 2006).

Several research efforts have been presented in the last years, focusing on the investigation of the structural response of masonry arches. Different techniques have been developed, ranging from a quick estimation of the ultimate strength to a more refined or exact evaluation of the mechanical response. In more sophisticated numerical models, details of damage like cracks can be observed. In (Motsa et al., 2020), a finite element model with unilateral interfaces is developed to predict failure in Mnajdra megalithic monument. In (Drosopoulos et al., 2008), unilateral contact-friction laws were used to simulate potential failure of a stone arch bridge due to various loads including settlement of supports and concentrated live load. A multi-scale model has been proposed in (Drosopoulos and Stavroulakis, 2018) adopting the extended finite element method to capture arbitrarily oriented cracks and localization phenomena in masonry structures. More efforts on numerical modelling of masonry structures using the finite element method can be found in

* Corresponding author. Technical University of Crete, School of Production Engineering and Management, GR-73100, Chania, Greece.
E-mail address: gestavr@dpem.tuc.gr (G. Stavroulakis).

[1] The research was partially funded by a cooperation project between the Greek Ministry of Culture and Sports, The Region of Crete, The Municipality of Chania and the Technical University of Crete (Contract ID 20SYMV007057887 2020-07-21).

https://doi.org/10.1016/j.dibe.2022.100069
Received 9 November 2021; Received in revised form 31 January 2022; Accepted 17 February 2022
Available online 24 February 2022

Fig. 1. The Neoria monument (Providakis, 2021).

(Betti et al., 2016; Conde et al., 2016; Stavroulaki et al., 2018).

In the present paper, the structural analysis investigation of the Neoria masonry vaulted structure at the Venetian harbor of Chania is presented (Fig. 1). Data related to the structure, the material, the damages and the foundation have been collected during a recent research project (Providakis, 2021). The accurate representation of the geometry of the vaults and the spandrels is necessary in order to model the existing condition including permanent deformations, loose material, cracks (Stavroulaki et al., 2016). This is important for the estimation of the structural strength and dynamic behavior considering the three dimensional, effects of the vaults and the stabilization role of the spandrels (Stavroulaki and Tsinarakis, 2011).

Two different approaches are reported here for the explanation of existing cracks and damages in the Neoria structure. First a classical modal analysis procedure is followed and the areas of higher deformation in the structure are correlated with damage patterns. Furthermore, two- and three-dimensional models with unilateral interfaces are used in a push-over like analysis, to investigate collapse modes and loads. Eigenmodal results are compared to measured data (Providakis, 2021). The procedure has been supported by Python-driven modelling and optimization. Finally, an initial effort is presented, towards the investigation of damage using a three-dimensional non-linear Extended Finite Element Method (XFEM) model. The results indicate the difficulty of this inverse analysis task, in view of the many uncertainties of monuments and must be evaluated carefully, since pushover analysis has been developed mainly for ductile frame structures, while unreinforced masonry has limited, practically zero ductility.

2. Modelling and linear analysis of the structure

2.1. Description of the structure

The Neoria are shipyards built in the 16th century for the repair of the venetian fleet. The front (north) facade was originally open for the entry of the ships. The southern walls were constructed and connected to the lateral walls up until the base of the vaults. Neoria reached about 50 m in length and 9 m of width for each shipyard. The construction of the Neoria is of cut stones up until a height of about 2.5 m and rubblework for the rest of the mass of the walls and the vaults. It is assumed that a destructive earthquake in the 19th century caused serious damages to the structure. The parts of the walls that collapsed, mainly in the southern façade, were filled with smaller rocks. The buttresses were constructed during that period. The walls of the north façade were built in the early 20th century. During the World War II, two vaults were partly destroyed. Last interventions are mainly related to the repair of the two damaged vaults and the application of waterproofing materials (Skoutelis et al., 2021).

2.2. Geometric modelling

Existing drawings have been updated and enriched thorough new measurements (Providakis, 2021). This resulted to a fully three-dimensional model with adequate details able to support structural analysis (Fig. 2 (a) – (e)). Specific areas with different material properties, as shown in Fig. 2(a)–(e), were assumed.

About the material properties, the masonry walls and the vaults have been investigated by using various destructive and non-destructive testing techniques. Additional literature investigation provided us with values for the same or similar monuments in the area (see Table 1).

Rigid constraints have been assumed for the foundation. Foundation settlements have not been observed or reported, apart from possible local influence at the vicinity of newly constructed saw-water installations near the north-west corner of the monument. In addition, the walls of south and north part are based on the soil at the level of the ground. They have been added to the structure after the construction of the vaults and they are no bearing structural elements. Nevertheless during earthquake loading or eventually settlement of supports, they cooperate with the other parts of the structure, acting in some sense like infills. In addition, the bearing parts of the structure that are based on a lower level are also fixed and supported due to the surrounding soil. Therefore this simplified assumption related to the foundation of the walls does not influence the results, at list for the preliminary investigation reported here. Soil-structure interaction will be considered in more details later for detailed analysis.

2.3. Finite element static and modal analysis

Various finite element models have been created. A typical model has 117308 number of nodes and 67766 number of three-dimensional hexahedral elements. Indicative static analysis results are shown in Fig. 3.

Some of the calculated eigenvalues and eigenmodes of the Neoria structure are shown in Fig. 4 (a) – (f).

The eigenmodal participation factors are shown in Fig. 5 (a,b) in the two directions of the structure. From the modal analysis it turns out that there are frequencies where the vaults develop oscillation in the longitudinal direction and that is taken into account in a three-dimensional simulation and analysis of the structure. Specifically in Fig. 4, the oscillation of the vault of the western neorio in the 6th, 24th and 25th eigenmodes, is shown.

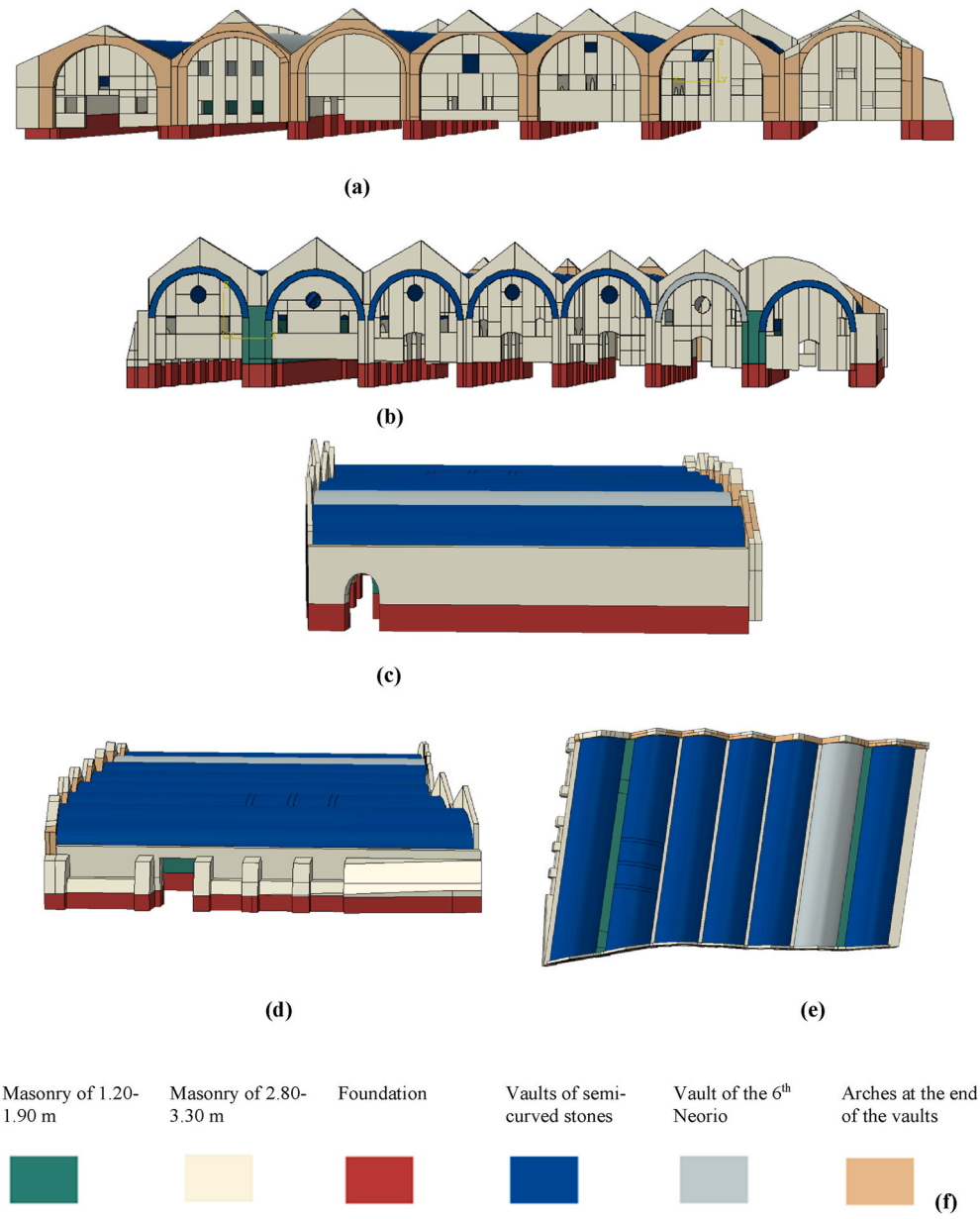

Fig. 2. (a) North view of the model, (b) south, (c) east, (d) west and (e) above view, with colors indicating areas of different material properties. (f) Colors assigned to various structural parts. (For interpretation of the references to color in this figure legend, the reader is referred to the Web version of this article.)

Table 1
Material properties (Evlogimenou).

Parts of the structure	Modulus of Elasticity
Vaults of semi-carved stones, strong mortar and mean thickness of 0.80 m	1860 MPa
Arches of the end of the vaults, in the north, with carved stones, strong mortar and mean thickness of 0.60–0.65 m	2790 MPa
Longitudinal masonry of 1.20–1.90 m thickness, with carved stones in the outer layers and strong mortar	504 MPa
Longitudinal masonry of 2.80–3.30 m thickness, with carved stones in the outer layers and strong mortar	340,2–3000 MPa
6th Neorio vault with shotcrete layer and π shaped hooks.	3280 MPa
Poisson ratio	0.20
Stone weight	21 kN/m3

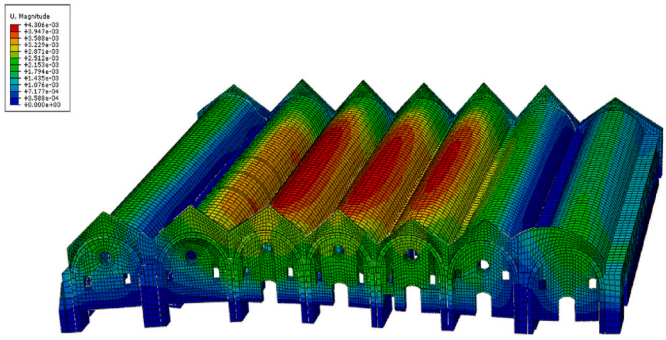

Fig. 3. Displacement for gravity loads (static load).

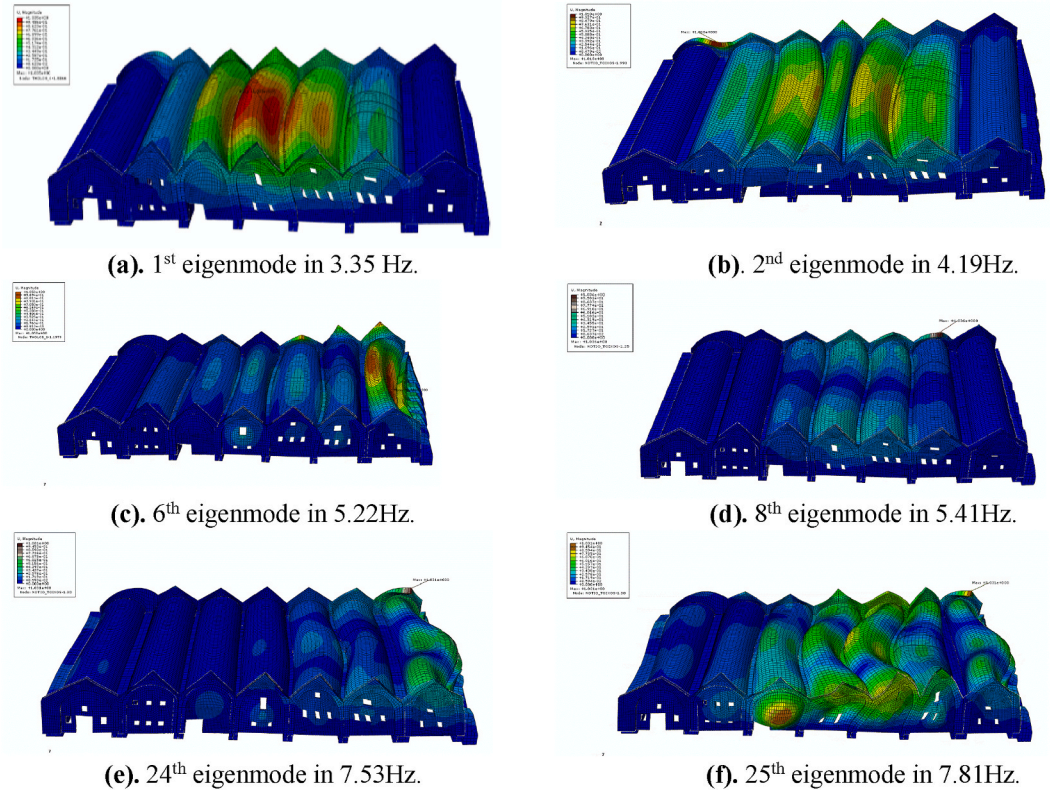

Fig. 4. Selected eigenmodes of the structure.
(a). 1st eigenmode in 3.35 Hz. **(b).** 2nd eigenmode in 4.19Hz.
(c). 6th eigenmode in 5.22Hz. **(d).** 8th eigenmode in 5.41Hz.
(e). 24th eigenmode in 7.53Hz. **(f).** 25th eigenmode in 7.81Hz.

Models in various commercial finite element codes have been prepared (MARC, ABAQUS, NX), with no significant differences.

It must be noted that recent design guidelines KADET 2021 (Regulation for valuation, 2021) require that at least 75% of the active mass must be considered in the modal analysis procedure. For the studied structure this requirement leads to the need of taking into account 142 modes (in X direction) or 197 modes (in Y direction) to the eigenmodal analysis. The first 20 eigenvalues are given in Table 2. From experimental measurements and the picture of existing damages it can be estimated that the structure experienced in the past seismic actions that activated eigenmodes near the value of 15 Hz.

It should be mentioned here that according to the provisions of KADET one observes that in the present structure, which does not have diaphragms, the modal analysis using as many eigenvectors as are required in order to activate the 75% of the total mass requires the inclusion of many eigenmodes. Alternatively, it is recommended to use the time-history analysis, by using a number of characteristic time series representing earthquakes expected in the region (following KANEPE sect. 5.6.3.3). In this paper the dynamic identify of the structure and material/damage identification is performed. For aseismic design and restoration design spectral analysis vs. time-series earthquake loading must be considered and performed. Comparison of the two approaches will be presented in the future.

Further investigation includes the introduction of cracks and soft interfaces at places where such damages have been found (Lakzaeian, 2011). The model with cracks and interfaces and the results are reported in (Charalambidi et al., 2021).

2.4. Parametric modelling and parameter identification

Due to the uncertainty which occurs mainly in material properties and damage patterns, several combinations of inputs must be considered in the mechanical model. The finite element models have been parametrized and driven through a Python script. Eventually, the model will provide the eigenmodes and eigenvalues near to the experimentally measured ones.

The parametrized model has different material properties assigned to different parts of the structure. Theoretically, every combination of elastic material properties can be considered. Based on the reliability of experimental measurements, the final investigation restricted the number of unknown parameters to three, within reasonable intervals for their values (Fig. 6).

The final step is composed of 512 combinations of parameter values and the calculated eigenmodes and eigenvalues. The calculated eigenmodal parameters have been compared with experimental measurements. The first criterion was the deviation between the calculated and the experimental eigenvalues. The Modal Assurance Criterion (MAC) has been supplementary used in order to assure that the compared modes are correctly chosen. MAC values show the convergence between numerical and experimentally measured eigenvalues. The closest this value to one, the better the correlation. This procedure is suitable for massive, monumental structures with complex-shaped eigenmodes and densely placed eigenvalues (Charalambidi et al., 2021) and (Asikoglu et al., 2019). The best combination of material parameters is shown in Table 3. The first row in Table 2 contains the experimentally measured eigenfrequencies (Providakis, 2021). The identification of predominant combinations by MAC is shown in Fig. 7. Different combinations of MAC for values greater than the threshold of 0.3 are presented.

The relation between the experimentally measured eigenfrequencies and the calculated eigenfrequency values is depicted in Fig. 8. The correlation between the MAC coefficient with the numerical eigenfrequencies and the difference between experimental and numerical

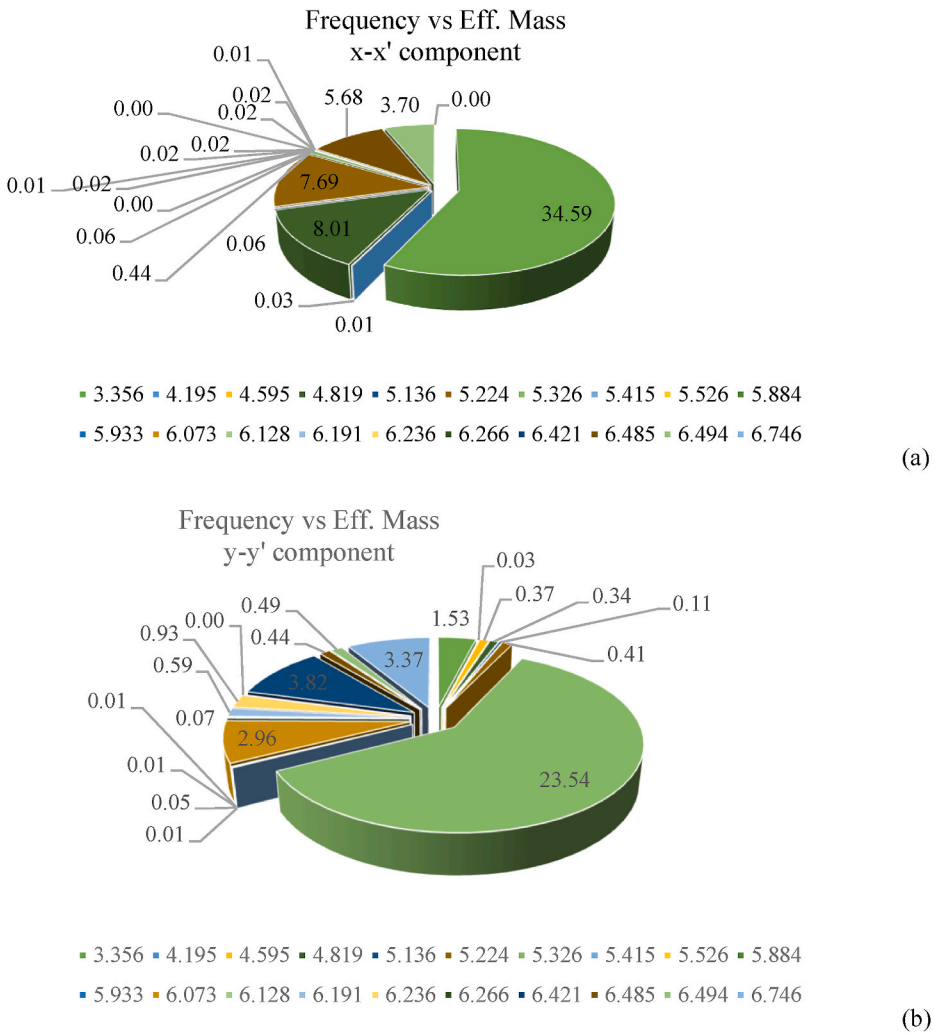

Fig. 5. Eigenmodal participation factors for earthquake in X and Y direction.

eigenfrequencies with the numerical eigenfrequencies is shown in Fig. 9.

In contrast to other works, which consider experimental data from the sterile laboratory environment or study relatively flexible structures (bridges, towers, belltowers, minarets etc), the achieved MAC values are relatively small. For general information and critical appraisal of various MAC factors the reader is referred to (Allemang, 2003) and (Pastor et al., 2012).

3. Pathology of the structure

For the structural model optimization, an analytical investigation of structure's damages was conducted. The purpose of the investigation was to include the existing deteriorations in the finite element model. The identified deteriorations are both biological (perforation, powdering) and mechanical (cracks, previous interventions with incompatible materials). The most important deteriorations of those detected were chosen to be included in the structural model. In Fig. 10, selected areas are illustrated that were simulated as regions of reduced stiffness, that is, three cracks observed in between the buttresses on the west wall, the large width cracks on vaults and the diversity of the width of the southern wall in the 7th Neorio. A longitudinal crack was recorded on the western vault. Because of its small width, it was not included in the analysis.

The structural conditions of the 4th and 6th vault from the west due to poor interventions are also considered as important (Fig. 11 (a)-(b)). They have been imported to the model as material with reduced strength (reduced elastic modulus).

Large width cracks of the inside of the vaults and on the west wall are illustrated in the followed Figures (Fig. 12 (a) – (c))

4. Unilateral crack models and non-linear analysis

4.1. Preliminary structural analysis modelling with cracks

From the in-situ investigation, the crack patterns have been documented. The finite element model of the structure (Ferrari et al., 2019) has been enhanced with weak zones that model, in a simplified way, the existence of cracks and other damages. In Fig. 13, the simulation of the critical cracked region of the structure are illustrated via proper partitioning of the finite element model.

From the analysis and the experimental investigation, it has been shown that higher vibration is accumulated near the frequency of 15 Hz. Therefore, the correlation of existing cracks with the maximum deformation patterns is shown in Fig. 14.

4.2. Classic limit state analysis

A limit state analysis was carried out using LimitState:Ring (Ferrari et al., 2019). Namely, a parametric analysis carried out to check the sensitivity of the ultimate load due to the number of masonry stones that make up one arch, as well as due to the estimated coefficient of friction between the masonry stones. It should be noted that the reason for

Table 2
Eigenvalues for various combinations of materials in the three areas.

Material - Modulus of Elasticity (Pa) (10^9)			7.06 Hz		11.56 Hz		15.75 Hz		17.62 Hz		18.5 Hz		24.62 Hz	
No1	No2	No3	*MAC* (10^{-4})	*f(Hz)*	*MAC*	*f(Hz)*	*MAC*	*f(Hz)*	*MAC*	*f(Hz)*	*MAC*	*f(Hz)*	*MAC*	*f(Hz)*
3,00	2,00	3,75	7,20	7,54	0,21	11,74	0,37	17,20	0,29	17,21	0,34	17,21	0,31	23,71
3,00	2,00	4,00	7,10	7,54	0,22	11,76	0,36	17,24	0,31	17,24	0,33	17,24	0,28	23,23
3,00	3,50	3,50	8,40	7,51	0,26	10,25	0,12	16,60	0,40	18,41	0,40	18,41	0,41	23,82
3,00	3,50	4,00	9,20	7,51	0,26	10,42	0,11	16,63	0,31	18,52	0,30	18,52	0,43	23,88
3,25	2,00	3,75	6,50	7,55	0,21	11,8	0,22	15,86	0,33	19,09	0,33	17,29	0,32	23,6
3,25	3,50	3,00	7,20	7,51	0,29	10,18	0,15	16,67	0,33	18,44	0,34	18,44	0,43	23,77
3,25	3,50	3,25	7,30	7,51	0,29	10,26	0,14	16,70	0,30	18,51	0,31	18,51	0,54	23,87
3,25	3,50	3,75	6,90	7,51	0,27	10,43	0,13	16,73	0,39	18,60	0,40	18,60	0,46	23,98
3,50	2,50	3,50	4,00	7,62	0,2	10,67	0,25	16,94	0,36	16,94	0,32	18,58	0,39	23,27
3,50	3,00	3,00	4,70	7,11	0,08	11,17	0,11	17,17	0,36	17,71	0,32	17,71	0,34	23,37
3,50	3,50	3,00	5,30	7,51	0,3	10,26	0,15	16,77	0,31	18,62	0,24	18,62	0,50	23,87
3,50	3,50	3,50	4,40	7,53	0,28	10,42	0,08	16,83	0,32	18,76	0,31	18,76	0,44	24,01
3,75	2,50	3,50	3,20	7,62	0,19	10,71	0,21	17,13	0,35	17,01	0,30	18,69	0,44	23,35
3,75	2,50	4,00	4,20	7,6	0,2	12,88	0,34	17,24	0,29	17,24	0,34	17,24	0,31	23,69
3,75	3,00	3,00	4,90	7,48	0,1	11,21	0,1	17,24	0,36	17,81	0,30	17,81	0,36	23,4
3,75	3,00	3,75	5,80	7,49	0,27	10,21	0,11	17,20	0,36	18,03	0,34	18,03	0,31	23,5
3,75	3,50	3,00	4,70	7,54	0,32	10,32	0,10	16,86	0,41	18,72	0,36	18,72	0,46	23,94
3,75	3,50	3,25	4,50	7,56	0,29	10,41	0,14	16,9	0,45	18,79	0,40	18,79	0,45	24,01
3,75	3,50	3,50	4,20	7,57	0,28	10,49	0,13	16,93	0,30	18,85	0,32	18,85	0,42	24,08
3,75	3,50	3,75	4,40	7,66	0,27	10,58	0,06	16,92	0,41	18,93	0,34	18,93	0,37	24,14
3,75	3,50	4,00	4,70	7,66	0,19	10,68	0,10	16,95	0,41	19,00	0,35	19,00	0,35	24,19

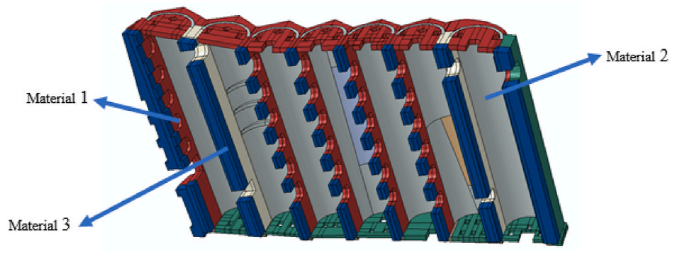

Fig. 6. Identification of parameters in selected areas, according to the instructions of the sensitivity analysis.

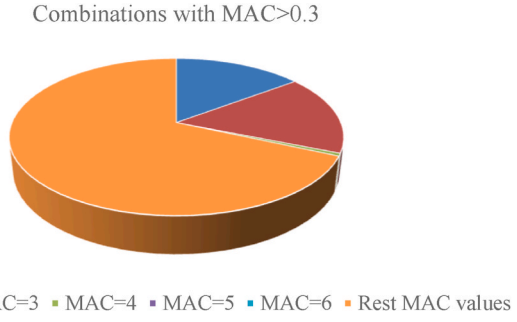

Fig. 7. Identification of predominant combinations by MAC. Percentage of cases with 2,3 etc MAC values greater than the threshold.

Table 3
Geometrical parameters of the damaged arch (west arch).

Shape of intrados	Span (m)	Rise at mid Span (m)	Thickness (mm)	Total Width (m)	Number of units
Segmental	9.39	4.695	727	5.0	20

considering only one arch in these simulations, is primarily to provide an indication for the number of blocks which can be used for each arch in the subsequent cases as well as to suggest a prediction for the friction coefficient. Thus, these simulations are only preliminary and cannot be used for in-depth evaluation of the structural response.

Table 3 shows the geometrical parameters of the arch on the west side which was used for the analysis, since it is the most damaged and it is expected that it will provide a better sense of the condition of the structure.

For the parametric analysis models, a 1 kN load was applied across the span of the arch at 150 mm intervals to identify the critical failure load of the arch and the position it is obtained. The results from the parametric analysis are shown in Figs. 15–16.

From the parametric analysis, it can be observed that failure load increases, until coefficient of friction reaches the value 0.47. The critical load observed is 87.9 kN when the number of segments is set to 10. From previous studies, it has been shown that the assumed coefficient of

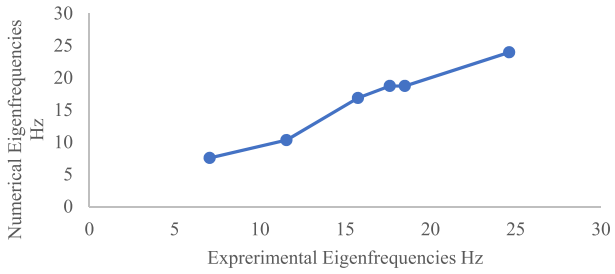

Fig. 8. Correlation between experimentally measured and calculated eigenfrequencies.

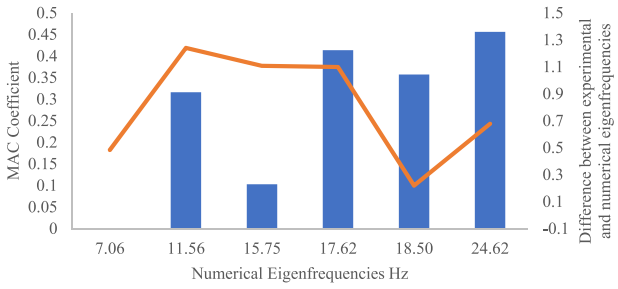

Fig. 9. Correlation between MAC coefficient (blue bar) and difference between experimental and numerical eigenfrequencies (orange line) with numerical eigenfrequencies. (For interpretation of the references to color in this figure legend, the reader is referred to the Web version of this article.)

friction between the masonry blocks tends to give the upper bound of the critical failure load if not coincide with the exact value of failure (Limitstate, 2021). Therefore, for the rest of the models, a 0.5 coefficient of friction has been adopted.

In the next step, the number of masonry blocks that make up the ring were investigated to determine the point at which the number of blocks has no significant effect on the failure load. It can be noted from Fig. 15, that the critical load decreases with the increase in the number of blocks until 10 blocks, whereby the critical load shows a lot of noise. However, when the average of the corresponding critical load from 3 consecutive blocks is plotted, the noise in the critical load becomes insignificant after 20 blocks are used to make up the arch. Therefore, for the rest of the models, each arch is made up of 20 masonry blocks.

It is noted that the failure mechanism obtained from the parametric models, correlates to the longitudinal cracks that were observed on the first arch as mapped on Fig. 10. The mode of collapse is a four-hinge failure mechanism as shown in Fig. 16.

4.2.1. *Two-dimensional analysis*

The mechanical behavior of unreinforced masonry structures is mainly based on compression loads transferred between adjacent parts of it, for instance stones, and secondary on frictional effects. This behavior is also known as unilateral, no-tension behavior. The existence of mortar with unreliable and low tensile strength is neglected. A further simplification for slender structures, like arches or domes, is based on the introduction of unilateral contact interfaces that model the nonlinear behavior. The activation or deactivation of contact, eventually with friction, during loading lead to reduction of the strength of the structure and eventually collapse, due to the formation of collapse mechanisms.

Following this method developed in our previous work (Drosopoulos et al., 2008; Gilbert and Melbourne, 1994) and (Du, 2019) for masonry bridges, a two-dimensional model for one arch as well as for the seven arches of Neoria in the East-West direction has been created. A number of unilateral contact interfaces are included. By applying a horizontal or

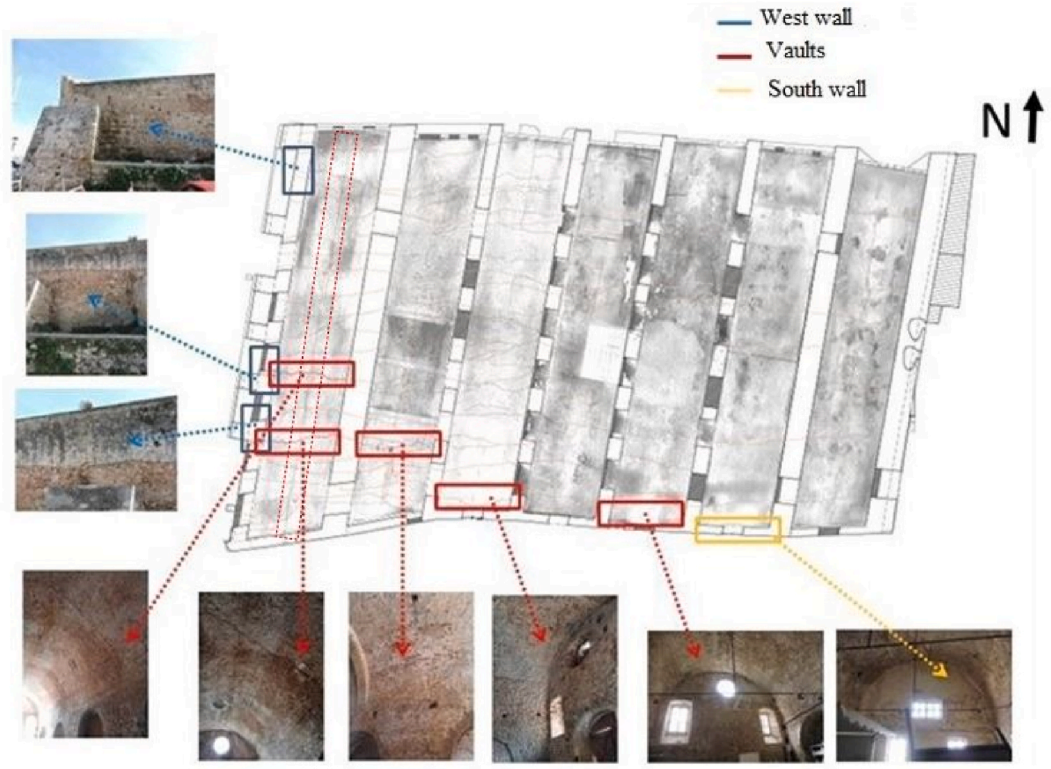

Fig. 10. Areas of reduced ductility on the vaults and on the walls of the structure.

(a) (b)

Fig. 11. Vault (a) inside and (b) outside view.

(a) (b)

(c)

Fig. 12. Crack on vault. (a) Inside and (b) outside view. (c) Biological deterioration on the North Wall.

vertical live load and gradually increasing it, similar to push-over analysis, the unilateral interfaces are activated and eventually collapse is modeled.

Careful application of this procedure, which is recommended by modern design regulations for ductile structures, gave crack patterns that partially explain the measured crack patterns at the outside walls of the structure. A vertical push-down procedure is followed for the estimation of the vertical component of the earthquake on a two-dimensional model of the single, west arch. Thus, the applied load combination consists of the self-weight, assigned in a first load step and an increased by 0.5g vertical gravity load, assigned in a second load step. Activation of cracks at the crown of the vaults can be explained by this procedure. Crack patterns at the west part of the structure can be correlated with the results of the full seven-openings model.

It must be repeated here that the results of pushover analysis have been used to give indicative correlation with existing crack patterns. Due to lack of ductility of the unreinforced masonry structure, they cannot be used for strength evaluation. From the collapse type and the

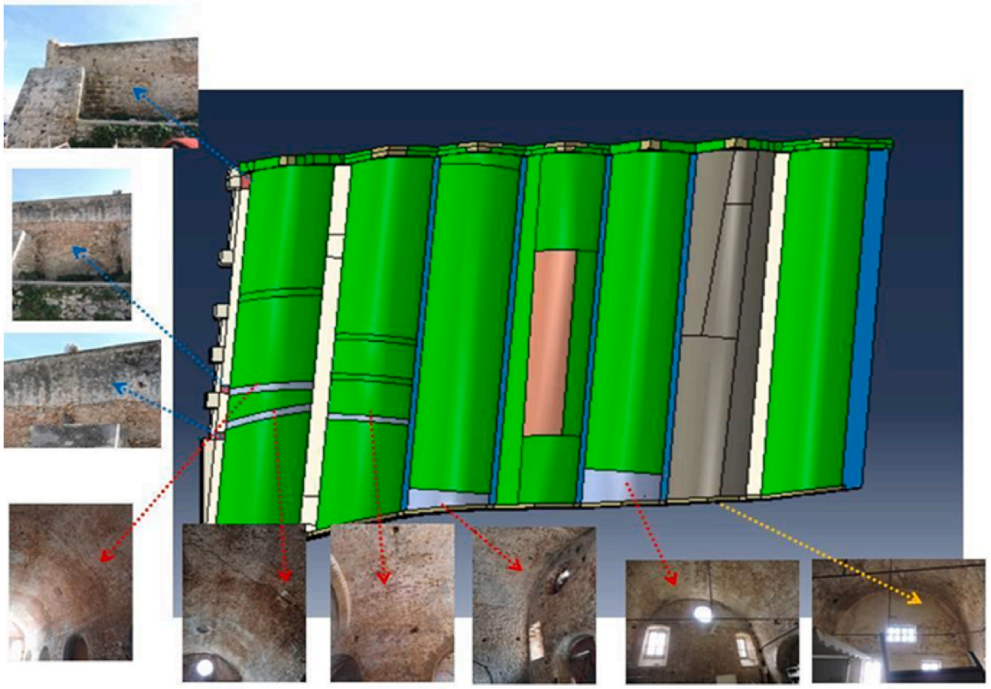

Fig. 13. Simulation of cracked region via partitioning of the F.E. model.

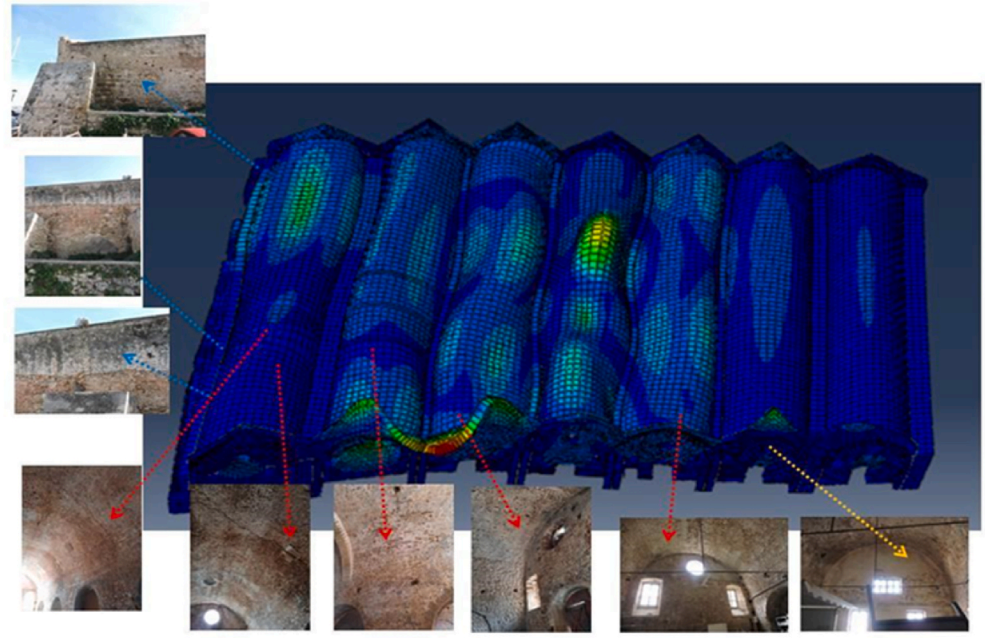

Fig. 14. 15 Hz eigenvalue shape of the structure (cracked model).

performance of the overall two-dimensional model it is observed that the most vulnerable areas are the extreme vaults (Fig. 17). Pathology observation indicates the appearance of longitudinal cracks in the vault of the western and eastern Neorio. These cracks have caused the key vault to break on the north front. It is pointed out that there is no immediate risk of collapse as evidenced by the collapse mechanism which requires the development of cracks in other places of the vault as well as movement of the spandrels (longitudinal walls).

4.2.2. Three-dimensional analysis

Next, a three-dimensional non-linear finite element model is developed in Abaqus (Simulia, 2013). It is noted that comparing to limit analysis, the finite element models can provide more details such as the principal stresses, forces and displacements which can be translated to force-displacement diagrams.

The geometry shown in Table 4 was used to create the numerical models. The longitudinal support provided by masonry walls were also included in the models. The width of the structure is reduced to 3.5 m to simplify the analysis.

The finite element models developed in this paper are solved using the Newton-Raphson incremental-iterative procedure to deal with the nonlinear nature of the problem. The nonlinearity is due to the opening-

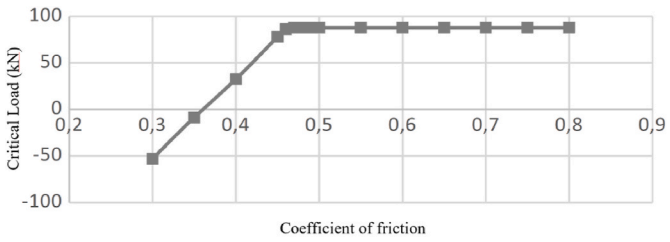

(a)

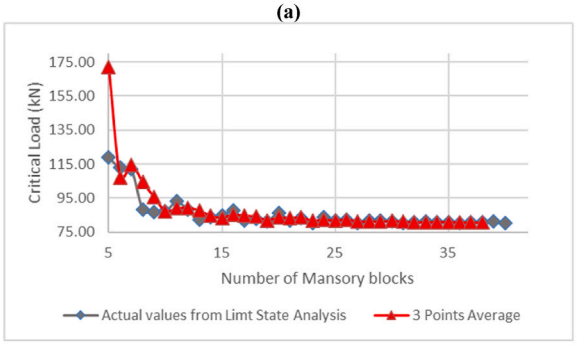

(b)

Fig. 15. Parametric analysis showing (a) the critical load vs the coefficient of friction between the masonry blocks and (b) the critical load vs the number of masonry blocks.

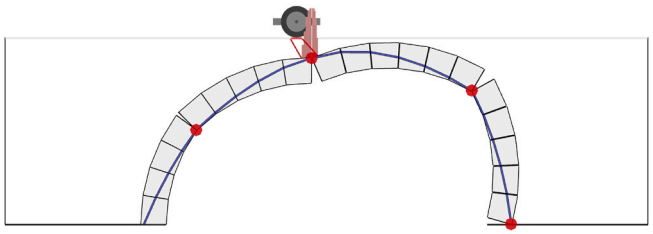

Fig. 16. The limit state failure mechanism of the first arch.

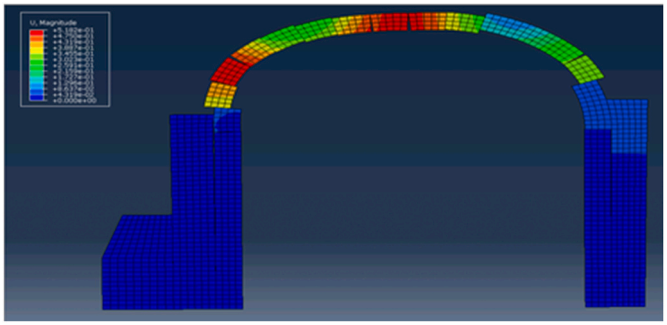

Fig. 17. Collapse mechanism (Western Neorio), where the activation of cracks in the center of the dome is clearly visible, as observed in the building.

closure and sticking-slipping along the masonry stone interfaces. The models were developed with a fixed support and the self-weight was incorporated in the loading condition. Two steps were used to create the models: the first step was a pure gravity load to simulate the state of inertia of the structure and to stabilize the model. The second step has an increased gravity load by 0,5g which was incrementally applied on the structure. This is used to provide a preliminary indication of the effect of the vertical component of an earthquake to the structural system. The results from these models are shown in Figs. 18–20.

The failure mechanism presented are shown in Figs. 18–20 correlate with the longitudinal cracks observed on the structure in-situ and the

Table 4
Maximum principal stresses (Maxps) used for XFEM model.

Material	Location	Maxps (MPa)
M1	Vaults with semi - carved stones, strong mortar and an average thickness of 0.80 cm	0.774
M2	Arches ending in the north with carved stones and strong mortar (thickness 0.60–0.65 cm)	1.116
M3	Longitudinal masonry 1.20–1.90 m thick with carved stones in the outer layers and strong mortar	0.2016
M4	Longitudinal masonry 2.80–3.30 m thick with stones in the outer layers and strong mortar	0.136
M5	Neoria dome 6 with operation with shotcrete and hooks of shape p.	–

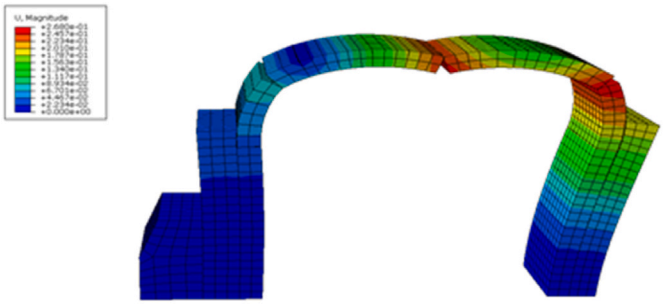

Fig. 18. The failure mechanism of the first arch under gravity loads.

damage pattern is similar to the one observed in the limit state analysis. Also, the model with one arch has a similar failure pattern with the full structure of 7 arches, even though the failure pattern is exaggerated on the one arch model. The hinge circled in yellow in Fig. 19 (model with one arch) and Fig. 20 (full structure) shows an outwards opening, respectively. For the model with the full structure, there is an influence of the adjacent arch to the first arch, which acts as a probe which prevents/minimize the lateral movement of the arch. This tends to minimize the overall displacement of the structure making it more stable.

After the first group of models with increased gravity of 0.5g were analyzed, it was noticed that the longitudinal cracks/opening only developed on the first (west) arch while on situ, also mapped on Fig. 10, longitudinal cracks are also visible in spans 2 and 7. In an attempt to understand the cause of the longitudinal cracks, more load cases were investigated:

- (a) Lateral movement of abutment due to a horizontal point load acting on the right-hand side abutment of the structure, as shown in Fig. 21.
- (b) A vertical displacement of supports.

Fig. 22 shows the deformation of the structure after a 100 kN horizontal point load has been applied on the right hand-side abutment. As shown on Fig. 22, multiple hinges (circled in red) are observed on the first span which correlates to the experienced damage. The yellow circles show small hinge opening on fourth, fifth and sixth spans. When the horizontal force is applied to the left hand-side abutment, no correlation to the experienced damage arises.

Figs. 23–24 show the deformation of the structure after imposing a 100 mm vertical (downwards) settlement of supports 2 and 8, as indicated by the red arrows. This movement of supports may be due to poor ground conditions. Fig. 24 highlights in red circles the hinge openings which might have resulted in the real cracks obtained in situ, as there is a high correlation of the positions of the cracks observed in the numerical model (Fig. 24) and in the real conditions (Fig. 10). The hinge opening on the fifth span (highlighted in yellow) is quite small, similar to the real

Fig. 19. The displacement contour of the whole structure under gravity loads.

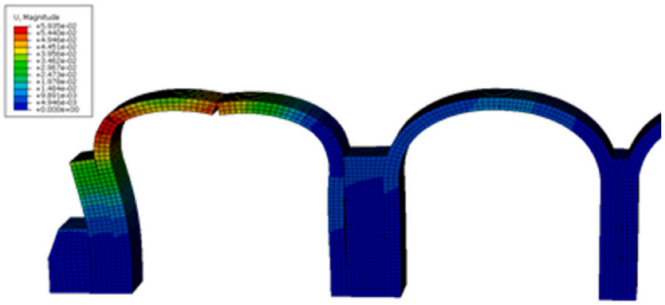

Fig. 20. A close-up view of the failure mechanism of the first arch in whole structure analysis under gravity loads.

Fig. 21. Lateral point load acting on the right-hand side abutment of the structure.

image. It can be concluded that the longitudinal cracks are most likely to be caused by a vertical displacement of supports 2 and 8.

4.3. Analysis with the extended finite element method

The extended finite element method (XFEM) is an extension of the conventional finite element analysis. It allows for cracks to be modeled independently of the mesh, permitting the propagation of the crack along an arbitrary, solution-based path (Du, 2019). The main concept of this method is to use the partition of unity property and properly enrich the nodal displacement approximation. The enrichment is implemented using appropriate enrichment functions, as provided by equation 2.

Within the XFEM method, a domain containing a discontinuity, is considered. This may involve a discontinuous displacement (strong discontinuity) or a discontinuous displacement gradient (weak discontinuity). A strong discontinuity can be used in numerical modelling to represent a crack, developed in a structure.

For a two-dimensional geometry, a strong discontinuity is depicted by a line located in the finite element mesh. According to the core concept of the XFEM method, the nodes of the elements which are cut by the discontinuity are enriched, using appropriate functions. These enrichment functions are used for the nodes of split elements (thus, elements which are cut by the discontinuity) and for the nodes of tip elements (elements which contain the crack tip). For the enrichment of the split elements, the Heaviside function H is used as given in equation (1). For the tip elements, the branch functions F are introduced.

$$u = \sum_{I=1}^{N} N_I(x)\left[u_I + H(x)a_I + \sum_{a=1}^{4} F_a(x)b_I^a\right] \tag{1}$$

For the structure that is investigated in this article, an XFEM model is developed in Abaqus (Du, 2019) to capture the transverse cracks. A simplified 3-dimensional geometry of the full structure is considered, similar to the full structure in the traditional FEA. A maximum principal stress (Maxps) is adopted to define the traction-separation law which is used to determine the response of the discontinuities. Crack propagation takes place when the stress in the domain of the crack tip reaches this maximum principal stress. Values of the Maxps for different elements of the structure are shown on Table 4. For all the cases, the displacement at failure was considered to be equal to 0.001 m. In this study, the initial

Fig. 22. (a) Deformation shape of first (west) span after a 100 kN horizontal point load has been applied on the right hand-side abutment, (b) Deformation shape of fourth, fifth and sixth spans after a 100 kN horizontal point load has been applied on the right hand-side abutment.

Fig. 23. Deformation shape of the structure after 100 mm vertical settlement of supports 2 and 8.

Fig. 24. (a) Deformation shape of 1st and 2nd span after 100 mm vertical settlement of supports 2, 8, (b) Deformation shape of 5th and 7th span after 100 mm vertical settlement of support 1, 8.

cracks were inserted on the first, second, third and seventh spans of the structure as observed on situ. For the mechanical conditions, a 100 mm vertical displacement of the second and eight support was applied together with a 100 kN horizontal force on the left abutment as shown on Fig. 26. The result from this model is shown in Fig. 26 (a)–(d).

Fig. 25(a) shows the initial position of the transverse cracks which are introduced to the model. According to the results of this investigation, the longitudinal cracks, which were observed on the conventional finite element analysis with similar load conditions, are also observed under the extended finite element model. In addition, based on this load case, as well as on more load cases including settlement of supports, analysis results indicate that the existing longitudinal cracks do not propagate. One potential reason for this, is the fact that these transverse cracks may not be considered as critical, since they will not interrupt the structural integrity of the system. Thus, in-between their positions, intact masonry arch parts will still be able to support the structural system.

However, further future investigation needs to be conducted, in order to provide more details for the interaction between longitudinal and transverse cracks and the influence of their interaction on the structural response.

5. Conclusions

Modal analysis results and pushover, limit analysis calculations have been used in order to explain damage and crack patterns found on the structure of the Neoria monument. First a three-dimensional finite element model was used for the classical modal analysis procedure and the areas of higher deformation in the structure were correlated with damage patterns.

The parametrized model has different material properties assigned to different parts of the structure. Theoretically, every combination of elastic material properties can be considered. Based on the reliability of experimental measurements, the final investigation restricted the number of unknown parameters to three, within reasonable intervals for their values (Fig. 20). From the reported investigation a fairly satisfactory determination of material parameters has been done, based on a detailed linear finite element model and experimental measurements. Further investigation may include parameter identification using multiple criteria and global optimization techniques. The Python script can support this, provided that sufficient computing time is available.

Furthermore, two- and three-dimensional models with unilateral interfaces were used in a push-over like analysis, in order to investigate collapse modes and loads. It is known that model with contact interfaces can be used in the stability assessment of a large monument (Motsa et al., 2019) and in combination with optimization for the investigation

Fig. 25. Deformation shape of the structure after a 100 kN horizontal point load has been applied on the further left hand-side abutment together with a 100 mm vertical displacement on the 100 mm vertical displacement of the second and eight support.

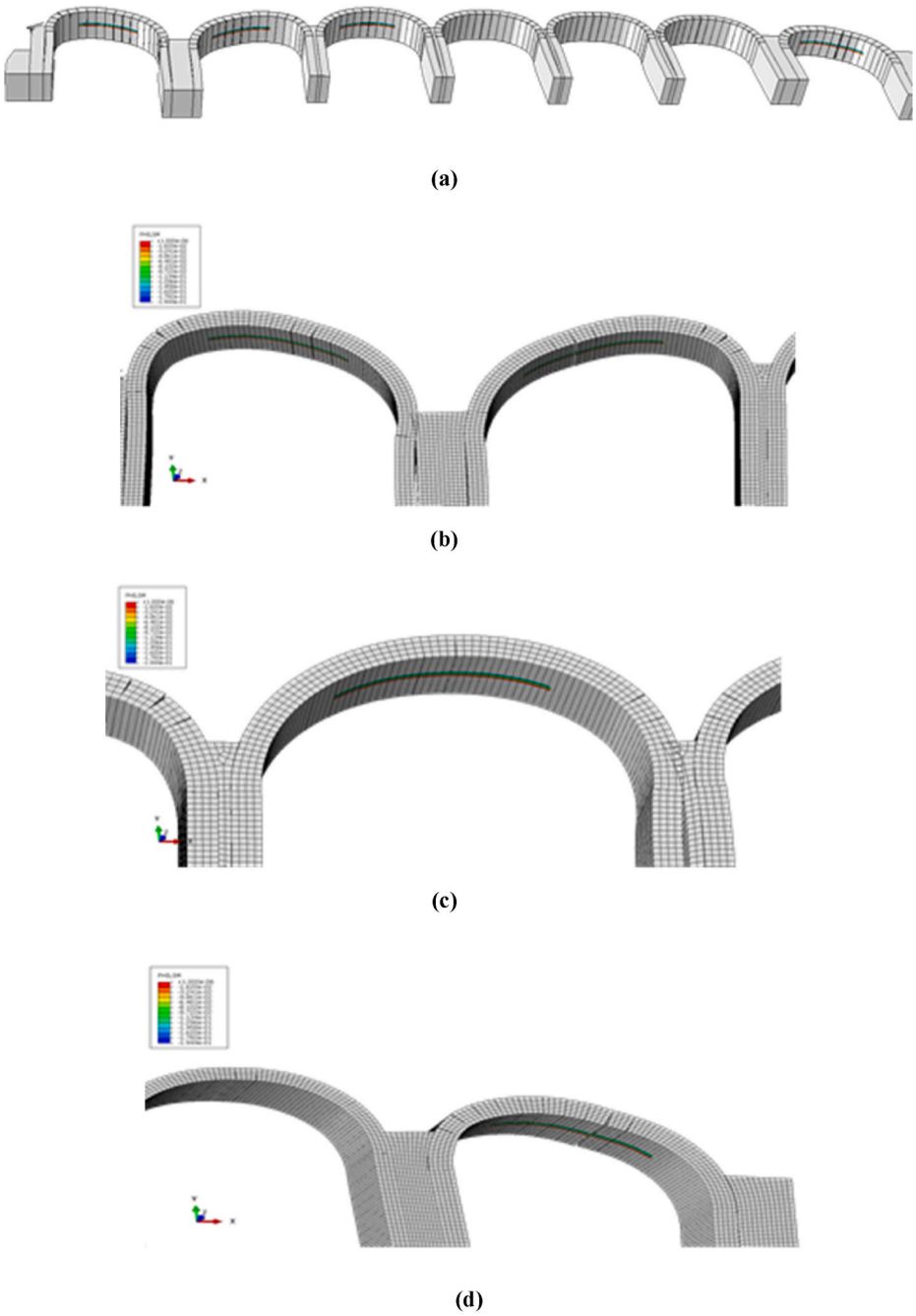

Fig. 26. (a) Transverse cracks on the different spans of the structure. Close-up (b) on the first and second span, (c) on the third span and (d) on the seventh span of the structure.

of structures with faults (Conde et al., 2016). Finally, the XFEM method was adopted to provide a further insight of the structural response, by considering transverse discontinuities.

From the analysis results it was concluded the important role of the west wall to the failures of the 1st Neorio vault. Additionally, the isolation of the masonry strength due to lack of maintenance as well as earthquakes are the main causes of existing failures. The understanding the mechanism of construction failure is basic to the next in studying the required interventions.

Due to the complexity of the structure, the uncertainties related to material properties, despite the extensive investigation, more work is needed, towards a further insight on crack propagation and reinforcement suggestions for the monument.

Declaration of competing interest

The authors declare that they have no known competing financial interests or personal relationships that could have appeared to influence the work reported in this paper.

References

Allemang, R.J., 2003. The modal assurance criterion – twenty years of use and abuse. Sound Vib. 37, 14–23. August.
Anastasio, S., 2020. Building between the Two Rivers: an Introduction to the Building Archaeology of Ancient Mesopotamia. Building between the Two Rivers. Archaeopress Archaeology, Oxford.
Asikoglu, A., Avşar, Ö., Lourenço, P.B., Kaplan, O., Karanikoloudis, G., 2019. Finite element modeling and operational modal analysis of a historical masonry mosque. In: Papadrakakis, M., Fragiadakis, M. (Eds.), 7th ECCOMAS Thematic Conference on

Computational Methods in Structural Dynamics and Earthquake Engineering Proceedings, Crete, Greece, 24–26 June.
Betti, M., Galano, L., Vignoli, A., 2016. Finite element modelling for seismic assessment of historic masonry buildings. In: D'Amico, S. (Ed.), Earthquakes and Their Impact on Society. Springer, Cham, pp. 377–415.
Charalambidi, B., Motsa, S., Drosopoulos, G., Koutsianitis, P., Kasampali, A., Stavroulaki, M., Stavroulakis, G., 2021. Structural damage investigation of the Neoria monument in Chania. In: 2nd International Conference TMM-CH. Athens.
Chilton, J.C., Isler, H., 2020. Heinz Isler: the Engineer's Contribution to Contemporary Architecture. Thomas Telford Publishing, Telford.
Conde, B., Drosopoulos, G., Stavroulakis, G., Riveiro, B., Stavroulaki, M., 2016. Inverse analysis of masonry arch bridges for damaged condition investigation: application on Kakodiki bridge. Eng. Struct. 127, 388–401.
Drosopoulos, G.A., Stavroulakis, G.E., 2018. A computational homogenization approach for the study of localization of masonry structures using the XFEM. Arch. Appl. Mech. 88, 2135–2152.
Drosopoulos, G., Stavroulakis, G., Massalas, C., 2008. Influence of the geometry and the abutments movement on the collapse of stone arch bridges. Construct. Build. Mater. 22, 200–210.
Du, Z.-Z., 2019. eXtended Finite Element Method (XFEM) in Abaqus. Simulia, Johnston.
Evlogimenou, I., December, 2011. Diploma Thesis. In: Venetian Neoria Chania: Static Solution and Intervention Proposal. NTUA, School of Architecture, D.P.M.S. Protection of Monuments.
Ferrari, R., Froio, D., Rizzi, E., Gentile, C., Chatzi, E.N., 2019. Model updating of a historic concrete bridge by sensitivity- and blobal optimization-based Latin Hypercube Sampling. Eng. Struct. 179, 139–160.
Gilbert, M., Melbourne, C., 1994. Rigid-block analysis of masonry structures. Struct. Eng. 72.
Heyman, J., 1982. The Mansonry Arch. Ellis Horwood Limited, Chichester.
Lakzaeian, F.H., 2011. Ambiend vibration testing and finite element model updating of a concrete footbridge. In: The 4th International Operational Modal Analysis Conference (IOMAC 2011). Istanbul, Turkey, 9-11 May.
Leftheris, B., Sapounaki, A., Stavroulaki, M.E., Stavroulakis, G.E., 2006. Computational Mechanics for Heritage Structures. WIT - Computational Mechanics Publications, Southampton, Boston.
Limitstate. Ring. https://www.limitstate.com/ring. (Accessed 23 October 2021).
Motsa, S.M., Drosopoulos, G.A., Stavroulaki, M.E., Stavroulakis, G.E., Ruben, P., Borg, P., Galea, P., d'Amico, S., 2019. Large-scale contact analysis for the stability estimation of the Mnajdra Monuments. In: Zigoni (Ed.), Advances in Engineering Materials, Structures and Systems: Innovations, Mechanics and Applications. Taylor & Francis, Abingdon, pp. 2160–2164.
Motsa, S.M., Drosopoulos, G.A., Stavroulaki, M.E., Maravelakis, E., Borg, R.P., Galea, P., D'amico, S., Stavroulakis, G.E., 2020. Structural investigation of Mnajdra megalithic monument in Malta. J. Cult. Herit. 41, 96–105.
Pastor, M., Binda, M., Harcarik, T., 2012. Modal assurance criterion. Procedia Eng. 48, 543–548.
Providakis, C., March 2021. Experimental investigation of eigenmodal characteristics. In: Skoutelis, N., et al. (Eds.), Research Investigation for the Restoration of Neoria, Technical University of Crete, Municipality of Chania, Ephorate of Antiquities. Chania.
Regulation for Valuation and Structural Interventions for Masonry (KADET), 2021. Greece.
Simulia, D.S., 2013. Abaqus 6.13 User's Manual. Dassault Systems, Providence, pp. 305–306.
Skoutelis, N., et al. (Eds.), March 2021. Research Investigation for the Restoration of Neoria. Technical University of Crete, Municipality of Chania, Ephorate of Antiquities, Chania.
Stavroulaki, M.E., Tsinarakis, Th, 2011. Finite element analysis of masonry barrel vaults. In: 7th GRACM International Congress on Computational Mechanics. Athens.
Stavroulaki, M.E., Riveiro, B., Drosopoulos, G.A., Solla, M., Koutsianitis, P., Stavroulakis, G.E., 2016. Modelling and strength evaluation of masonry bridges using terrestrial photogrammetry and finite elements. Adv. Eng. Software 101, 136–148.
Stavroulaki, M.E., Drosopoulos, G.A., Tavlopoulou, E., Skoutelis, N., Stavroulakis, G.E., 2018. Investigation of the structural behaviour of a masonry castle by considering the actual damage. Int. J. Mason. Res. 3, 1–33.